Arid1a is essential for intestinal stem cells through Sox9 regulation

Yukiko Hiramatsu[a], Akihisa Fukuda[a,1], Satoshi Ogawa[a], Norihiro Goto[a], Kozo Ikuta[a], Motoyuki Tsuda[a], Yoshihide Matsumoto[a], Yoshito Kimura[a], Takuto Yoshioka[a], Yutaka Takada[a], Takahisa Maruno[a], Yuta Hanyu[a], Tatsuaki Tsuruyama[b], Zhong Wang[c], Haruhiko Akiyama[d], Shigeo Takaishi[e], Hiroyuki Miyoshi[f], Makoto Mark Taketo[f], Tsutomu Chiba[g], and Hiroshi Seno[a]

[a]Department of Gastroenterology and Hepatology, Kyoto University Graduate School of Medicine, 606-8507 Kyoto, Japan; [b]Clinical Bioresource Center, Kyoto University Hospital, 606-8507 Kyoto, Japan; [c]Department of Cardiac Surgery, Cardiovascular Research Center, University of Michigan, Ann Arbor, MI 48109; [d]Department of Orthopaedics, Gifu University, 501-1194 Gifu, Japan; [e]Laboratory for Malignancy Control Research (DSK project), Medical Innovation Center, Kyoto University Graduate School of Medicine, 606-8507 Kyoto, Japan; [f]Division of Experimental Therapeutics, Kyoto University Graduate School of Medicine, Yoshida-Konoe-cho, Sakyo-ku, 606-8506 Kyoto, Japan; and [g]Kansai Electric Power Hospital, 553-0003 Osaka, Japan

Edited by Hans Clevers, Hubrecht Institute, Utrecht, The Netherlands, and approved December 13, 2018 (received for review March 21, 2018)

Inactivating mutations of *Arid1a*, a subunit of the Switch/sucrose nonfermentable chromatin remodeling complex, have been reported in multiple human cancers. Intestinal deletion of *Arid1a* has been reported to induce colorectal cancer in mice; however, its functional role in intestinal homeostasis remains unclear. We investigated the functional role of Arid1a in intestinal homeostasis in mice. We found that intestinal deletion of *Arid1a* results in loss of intestinal stem cells (ISCs), decreased Paneth and goblet cells, disorganized crypt-villous structures, and increased apoptosis in adult mice. Spheroids did not develop from intestinal epithelial cells deficient for *Arid1a*. Lineage-tracing experiments revealed that *Arid1a* deletion in Lgr5$^+$ ISCs leads to impaired self-renewal of Lgr5$^+$ ISCs but does not perturb intestinal homeostasis. The Wnt signaling pathway, including Wnt agonists, receptors, and target genes, was strikingly down-regulated in *Arid1a*-deficient intestines. We found that Arid1a directly binds to the *Sox9* promoter to support its expression. Remarkably, overexpression of *Sox9* in intestinal epithelial cells abrogated the above phenotypes, although *Sox9* overexpression in intestinal epithelial cells did not restore the expression levels of Wnt agonist and receptor genes. Furthermore, *Sox9* overexpression permitted development of spheroids from *Arid1a*-deficient intestinal epithelial cells. In addition, deletion of *Arid1a* concomitant with *Sox9* overexpression in Lgr5$^+$ ISCs restores self-renewal in *Arid1a*-deleted Lgr5$^+$ ISCs. These results indicate that Arid1a is indispensable for the maintenance of ISCs and intestinal homeostasis in mice. Mechanistically, this is mainly mediated by Sox9. Our data provide insights into the molecular mechanisms underlying maintenance of ISCs and intestinal homeostasis.

Arid1a | intestinal stem cell | homeostasis

Regulation of highly organized chromatin structure is essential for genomic stability, normal cellular growth, development, and differentiation (1–3). Epigenetic regulation is indispensable for establishing different degrees of chromatin compaction and conveying specialized gene-expression patterns that define the molecular basis of pluripotency reprograming, development, and homeostasis. Chromatin remodelers that disrupt DNA–protein contacts regulate gene expression (4). The Switch/sucrose nonfermentable (SWI/SNF) complex is one of the most extensively studied chromatin remodelers. The SWI/SNF complex contains a core ATPase (Brg1 or Brm) and noncatalytic subunits with various DNA-binding and protein-binding domains that influence targeting and activity of the complex. We recently reported that Brg1 plays an essential role in development and homeostasis of the duodenum through regulation of Notch signaling (5). On the other hand, loss of Arid1a, which directly interacts with DNA through a DNA-binding domain, disrupts SWI/SNF targeting and nucleosome remodeling, resulting in aberrant gene regulation (6, 7). In addition, a recent study showed that deletion of *Arid1a* in the intestines induces colon cancer in mice (8). However, the functional role of Arid1a in intestinal homeostasis and its underlying molecular mechanisms remain unknown.

Recently, studies with transgenic and knockout mice have elucidated the molecular mechanisms underlying the development of intestines as well as epithelial homeostasis and regeneration in adult intestines. Through these studies, several signaling pathways, including the Wnt, bone morphogenic protein, phosphatidylinositol-3 kinase, and Notch cascades, have been revealed to play critical roles in regulating cell proliferation and controlling stem cell self-renewal and differentiation in normal intestinal tissues. Notably, the Wnt pathway is crucial in a number of processes involved in intestinal development and homeostasis, including maintenance of stem cell identity, cell proliferation, secretory lineage differentiation, and epithelial segregation along the crypt-villus axis (9–13). Wnt3, which is produced specifically by Paneth cells (14, 15), is required for a stem cell niche in intestinal crypts (14) and for intestinal

Significance

The Switch/sucrose nonfermentable (SWI/SNF) chromatin remodeling complex plays critical roles for development and homeostasis of various organs. Intestinal deletion of *Arid1a*, a subunit of the SWI/SNF complex, has been reported to induce colorectal cancer in mice; however, its functional role in intestinal homeostasis remains unclear. This study reveals that intestinal deletion of *Arid1a* results in depletion of intestinal stem cells and disorganized crypt-villous structures concomitant with dramatically decreased expression of Sox9 in mice. Furthermore, our data reveal that Arid1a is indispensable for survival for intestinal stem cells and intestinal homeostasis through regulation of Sox9 expression in mice. These findings demonstrate an essential role of Arid1a to maintain tissue stem cells and homeostasis.

Author contributions: Y. Hiramatsu and A.F. designed research; Y. Hiramatsu, S.O., N.G., K.I., M.T., Y.M., Y.K., T.Y., Y.T., T.M., Y. Hanyu, H.A., and S.T. performed research; Z.W., H.M., and M.M.T. contributed new reagents/analytic tools; Y. Hiramatsu and T.T. analyzed data; and Y. Hiramatsu, A.F., T.C., and H.S. wrote the paper.

The authors declare no conflict of interest.

This article is a PNAS Direct Submission.

Data deposition: The data reported in this paper have been deposited in the Gene Expression Omnibus (GEO) database, https://www.ncbi.nlm.nih.gov/geo (accession nos. GSE110181 and GSE121658).

[1]To whom correspondence should be addressed. Email: fukuda26@kuhp.kyoto-u.ac.jp.

This article contains supporting information online at www.pnas.org/lookup/suppl/doi:10.1073/pnas.1804858116/-/DCSupplemental.

spheroid cultures (16). In addition, a Wnt/Tcf4 target gene, *Sox9*, which is expressed in intestinal crypts (17, 18), is required for the differentiation of Paneth cells in intestinal epithelium (14, 19, 20).

Here, we show that Arid1a is indispensable for the maintenance of intestinal stem cells (ISCs), a critical niche for ISCs including Paneth cells, and the intestinal crypt-villous structure in mice. Furthermore, our data show that these roles of Arid1a are mainly mediated by *Sox9*.

Results

Intestinal Deletion of *Arid1a* Results in Growth Impairment, Low Survival Rate, and Abnormal Intestinal Structures After 3 wk of Age. To examine the expression pattern of Arid1a in murine intestinal epithelium, we first performed immunohistochemistry (IHC) for Arid1a in wild-type mice. Arid1a was expressed in all intestinal epithelial cells from postnatal to adult stages (Fig. 1*A*). To investigate the possible role of Arid1a in intestinal development and homeostasis, we crossed transgenic mice carrying a *loxP*-flanked allele of *Arid1a* with *Villin-Cre* mice (21) to generate *Villin-Cre;Arid1a*$^{f/f}$ mice. There was no difference between *Villin-Cre;Arid1a*$^{f/f}$ mice and control *Arid1a*$^{f/f}$ littermates in terms of survival rate, body weight, and intestinal architecture until 3 wk of age (Fig. 1 *B–D*). However, after 3 wk of age, low survival rate and weight loss were observed in *Villin-Cre;Arid1a*$^{f/f}$ mice compared with the control *Arid1a*$^{f/f}$ mice (Fig. 1 *B* and *C*). Histological analysis revealed gross morphological changes in *Villin-Cre;Arid1a*$^{f/f}$ mice, including shortened villi and swollen crypts in the small intestine but not in the large intestine (Fig. 1 *E–I* and *SI Appendix*, Fig. S1*A*). Furthermore, these abnormal intestinal architectures were more pronounced after 5 wk of age in *Villin-Cre;Arid1a*$^{f/f}$ mice (Fig. 1*F*). To investigate when the morphological changes had occurred, we performed histological analysis at postnatal day (P) 10 and P17. Intestinal structures of *Villin-Cre;Arid1a*$^{f/f}$ mice were indistinguishable from control *Arid1a*$^{f/f}$ mice at P10 and P17 (*SI Appendix*, Fig. S1*B*).

In accordance with *Cre* activity, almost all intestinal epithelial cells had lost Arid1a expression in *Villin-Cre;Arid1a*$^{f/f}$ mice, as determined by IHC analysis (*SI Appendix*, Fig. S2*A*). In addition, quantitative RT-PCR (q-PCR) analysis demonstrated that *Arid1a* expression was significantly decreased in *Villin-Cre;Arid1a*$^{f/f}$ intestines compared with that in control *Arid1a*$^{f/f}$ intestines (*SI Appendix*, Fig. S2*B*). These results indicate that intestinal deletion of *Arid1a* results in low survival rate, growth impairment, and abnormal intestinal structure after 3 wk of age in mice.

Given that Arid1b, one of the subunits of the SWI/SNF complex with a DNA binding domain, has been shown to preserve residual SWI/SNF activity in ARID1A-deficient cancer cell lines (8, 22), we investigated the expression pattern of Arid1b in the proximal and distal small intestine and in the large intestine of *Villin-Cre;Arid1a*$^{f/f}$ and control *Arid1a*$^{f/f}$ mice. Arid1b was only faintly expressed in the proximal small intestine of *Villin-Cre;Arid1a*$^{f/f}$ and control *Arid1a*$^{f/f}$ mice, whereas it was expressed in the distal small intestine and the large intestine of *Villin-Cre;Arid1a*$^{f/f}$ and control *Arid1a*$^{f/f}$ mice, as determined by IHC analysis (*SI Appendix*, Fig. S3*A*). In addition, q-PCR analysis revealed that *Arid1b* expression was significantly higher in the distal small intestine and the large intestine compared with that in the proximal small intestine of *Villin-Cre;Arid1a*$^{f/f}$ and control

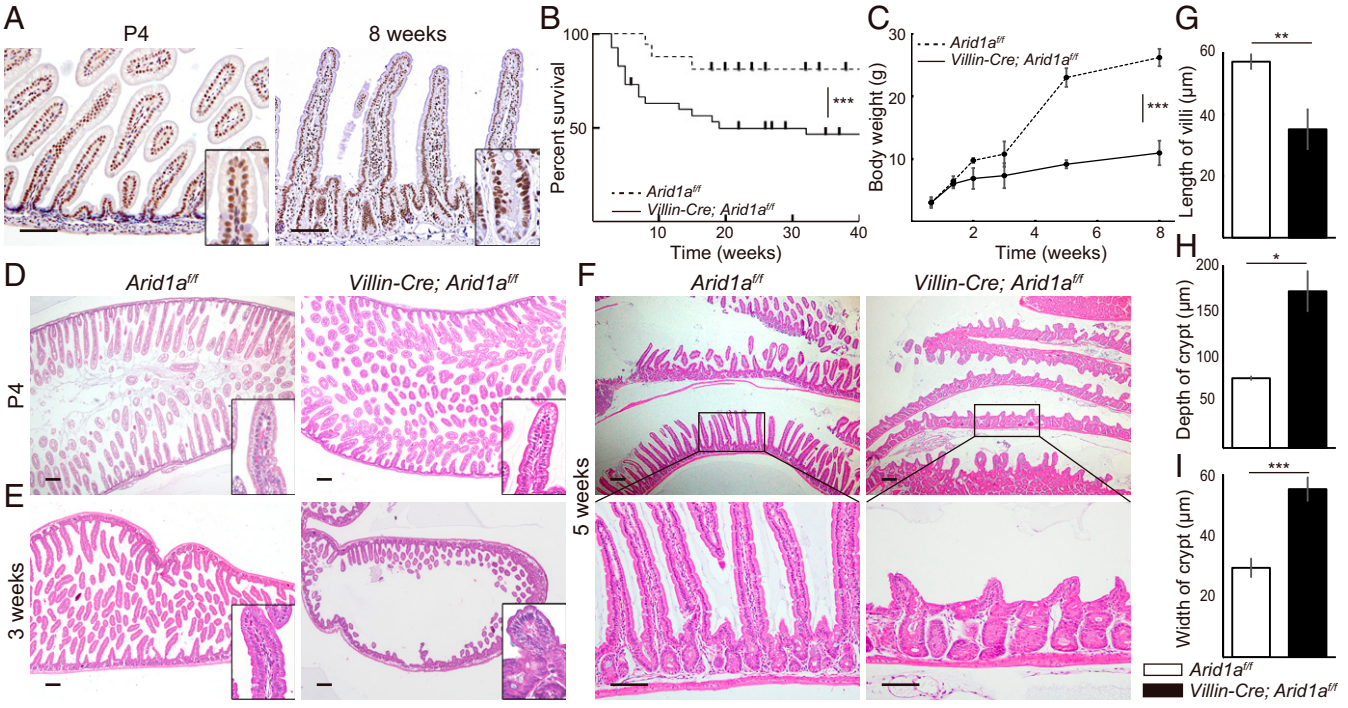

Fig. 1. Intestinal *Arid1a* deletion results in growth impairment, low survival rate, and abnormal intestinal structure in mice. (*A*) IHC for Arid1a in wild-type mice at P4 (*Left*) and at 8 wk of age (*Right*). (*B*) Kaplan–Meier survival curves show significantly lower survival rate ($P < 0.001$) in *Villin-Cre;Arid1a*$^{f/f}$ mice (line, $n = 30$) compared with control mice (dashed line, $n = 24$). (*C*) Body weight at indicated time points for control (dashed line, $n = 6$, male mice) and *Villin-Cre;Arid1a*$^{f/f}$ mice (line, $n = 6$, male mice). (*D–F*) H&E staining of the small intestines for control (*Left*) and *Villin-Cre; Arid1a*$^{f/f}$ mice (*Right*) at the indicated time points. There was no significant difference between control mice and *Villin-Cre;Arid1a*$^{f/f}$ mice at P4 (*D*). At 3 wk of age, the intestinal architecture of *Villin-Cre;Arid1a*$^{f/f}$ mice occasionally appeared to be abnormal compared with that in control mice (*E*). At 5 wk of age, disorganized intestinal architecture, including shortened villi and crypt enlargement, was constantly observed in *Villin-Cre;Arid1a*$^{f/f}$ mice (*F*). (*G–I*) Average length of villi (*G*), depth of crypts (*H*), and width of crypts (*I*) in control and *Villin-Cre;Arid1a*$^{f/f}$ mice at 8–10 wk of age ($n = 3$). [Scale bars, 100 μm (*A* and *F*) and 200 μm (*D–F*).] [*Inset* magnification, 2.7× (*A*) and 10× (*D* and *E*).] Quantitative data are presented as means ± SD, $*P < 0.05$, $**P < 0.01$, $***P < 0.001$.

Arid1a$^{f/f}$ mice, respectively (*SI Appendix*, Fig. S3*B*). These results suggest the possible compensatory role of Arid1b in the distal small intestine and the large intestine in *Villin-Cre;Arid1a*$^{f/f}$ mice.

Intestinal tumors were not observed in *Villin-Cre;Arid1a*$^{f/f}$ mice upon analysis at 65 wk of age (*SI Appendix*, Fig. S1*C*).

Intestinal Deletion of *Arid1a* Results in Skewed Differentiation in the Small Intestine. To investigate the effect of *Arid1a* deletion on the differentiation of small intestinal epithelia, we performed IHC analysis. Paneth cells that produce lysozyme and matrix metalloproteinase (Mmp)-7 were strikingly reduced in number in *Villin-Cre;Arid1a*$^{f/f}$ mice at 8–10 wk of age (Fig. 2 *A* and *B*). In addition, q-PCR analysis showed that the expression levels of Paneth cell markers—including *Mmp7* (23), *Lyz1*, and *Defa6* (14)—were significantly decreased in *Villin-Cre;Arid1a*$^{f/f}$ intestines compared with control *Arid1a*$^{f/f}$ mouse intestines (Fig. 2*C*). Alcian blue staining revealed that the number of goblet cells was also markedly decreased in *Villin-Cre;Arid1a*$^{f/f}$ mice (Fig. 2 *A* and *D*). However, the numbers of tuft cells and enteroendocrine cells in *Villin-Cre;Arid1a*$^{f/f}$ mice were comparable to those in control *Arid1a*$^{f/f}$ mice, as determined by quantification and immunostaining for Dclk1 (24) and chromogranin A, respectively (*SI Appendix*, Fig. S2 *C*–*E*). These results indicate that intestinal deletion of *Arid1a* results in reduced number of Paneth and goblet cells in the small intestine.

Intestinal Deletion of *Arid1a* Results in Increased Apoptosis in the Epithelial Cells of Small Intestines. To evaluate the cellular proliferation and apoptosis in the intestinal epithelial cells of *Villin-Cre;Arid1a*$^{f/f}$ mice, we performed immunostaining and quantification of K_i67 and cleaved caspase 3. The number of K_i67^+ cells in the disorganized crypts of *Villin-Cre;Arid1a*$^{f/f}$ mouse intestines was comparable to that of control *Arid1a*$^{f/f}$ mouse intestines at 8–10 wk of age (Fig. 2 *A* and *E*). In contrast, apoptotic cells were dramatically increased in the intestinal epithelial cells of *Villin-Cre;Arid1a*$^{f/f}$ mice. In control *Arid1a*$^{f/f}$ mice, few apoptotic cells were observed in the villi, but barely observed within crypts (Fig. 2 *A* and *F*). In contrast, *Villin-Cre;Arid1a*$^{f/f}$ mice demonstrated a number of apoptotic cells in crypts, as in the case of villi (Fig. 2 *A* and *F*). There were no significant differences in proliferation and apoptosis in the large intestine between *Villin-Cre;Arid1a*$^{f/f}$ and control mice (*SI Appendix*, Fig. S1 *A*, *D*, and *E*). These results demonstrate that intestinal loss of *Arid1a* results in increased apoptotic cells in both villi and crypts in adult mice.

To investigate the types of cells that showed apoptosis, we also performed a TUNEL assay. Apoptotic Lgr5$^+$ ISCs were detected by costaining for GFP and TUNEL in *Lgr5-GFP;Villin-Cre;Arid1a*$^{f/f}$ mice (*SI Appendix*, Fig. S4*A*), whereas there were no apoptotic Lgr5$^+$ ISCs in control mice. Because apoptotic cells were also increased in the villi of *Villin-Cre;Arid1a*$^{f/f}$ mice (Fig. 2*A*), we performed costaining for TUNEL or cleaved caspase 3 with various differentiated cell markers. Dual immunofluorescence staining demonstrated apoptosis in the enterocytes of *Villin-Cre;Arid1a*$^{f/f}$ mice, whereas apoptosis was not observed in other types of differentiated cells (*SI Appendix*, Fig. S4*B*). Collectively, these results indicate that apoptosis occurs in both Lgr5$^+$ ISCs in the crypts and enterocytes in the villi of *Villin-Cre;Arid1a*$^{f/f}$ mice.

To investigate whether electron microscopic changes occurred in enterocytes, including microvilli formation in *Villin-Cre;Arid1a*$^{f/f}$ mice, we next performed electronic microscopic analysis. We observed no differences in enterocytes in terms of microvilli formation, organelles, and nuclei between *Villin-Cre;Arid1a*$^{f/f}$ and control mice (*SI Appendix*, Fig. S2*F*).

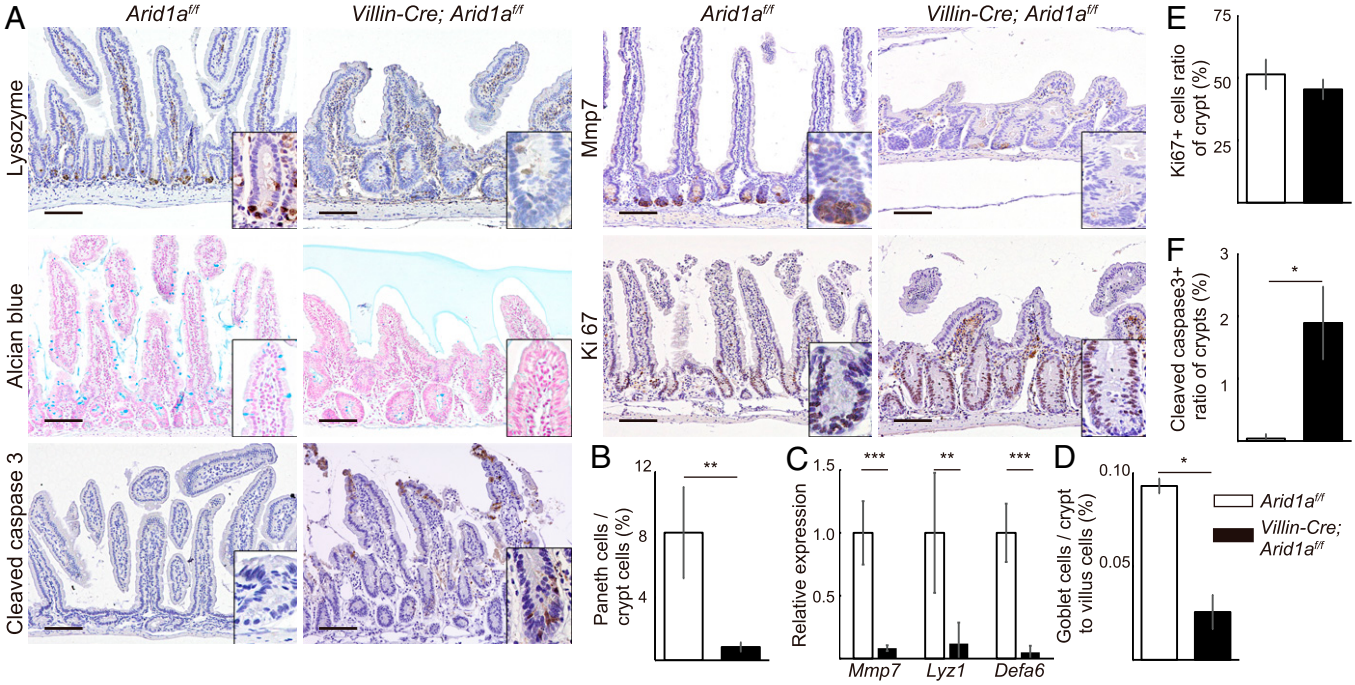

Fig. 2. Intestinal *Arid1a* deletion leads to decreased secretory cell lineages and increased apoptotic cells in the small intestines of mice. (*A*) IHC analysis for Lysozyme, Mmp7, Alcian blue, K_i67, and cleaved caspase 3 staining of the small intestines in control (*Left*) and *Villin-Cre;Arid1a*$^{f/f}$ mice (*Right*) at 8–10 wk of age. (Scale bars, 100 μm.) (*Inset* magnification, 2.7×.) (*B*) Ratio of the number of Paneth cells to crypt cells in control ($n = 5$) and *Villin-Cre; Arid1a*$^{f/f}$ mice ($n = 4$) at 8–10 wk of age. (*C*) Relative expression levels of Paneth cell markers in control and *Villin-Cre;Arid1a*$^{f/f}$ mice, as determined by q-PCR using crypt RNA at 8 wk of age ($n = 5$). (*D*) Ratio of the number of goblet cells to crypt to villus cells in control and *Villin-Cre;Arid1a*$^{f/f}$ mice at 8–10 wk of age ($n = 3$). (*E*) Ratio of the number of K_i67^+ cells to crypt cells in control and *Villin-Cre;Arid1a*$^{f/f}$ mice at 8–10 wk of age ($n = 3$). (*F*) Ratio of the number of crypts that contained at least one cleaved caspase 3$^+$ cell to all crypt numbers in sections from control and *Villin-Cre;Arid1a*$^{f/f}$ mice at 8–10 wk of age ($n = 3$). Quantitative data are presented as means ± SD, $^*P < 0.05$, $^{**}P < 0.01$, $^{***}P < 0.001$.

Arid1a Is Essential for the Maintenance of ISCs in Mice. To investigate the effect of *Arid1a* deletion in Lgr5$^+$ ISCs, we next crossed transgenic mice carrying a *loxP*-flanked allele of *Arid1a* with *Lgr5*$^{CreERT2/+}$ mice (25) to generate *Lgr5*$^{CreERT2/+}$*;Arid1a*$^{f/f}$ mice. Mice were intraperitoneally injected daily with 80 mg/kg of tamoxifen for 4 d. Three days after the last injection, IHC analysis revealed mosaic clusters of *Arid1a*-deficient cells in both crypts and villi of *Lgr5*$^{CreERT2/+}$*;Arid1a*$^{f/f}$ intestines (*SI Appendix*, Fig. S5*A*). However, 21 d after the last tamoxifen injection, the vast majority of intestinal epithelial cells including crypts were composed of Arid1a$^+$ cells in mutant mice (*SI Appendix*, Fig. S5*A*), and the intestinal architecture was normal. We also examined whether *Arid1a* deletion perturbs intestinal homeostasis at 1 and 2 wk after tamoxifen administration. We found that at 1 and 2 wk after tamoxifen injection, the intestinal architecture was normal (*SI Appendix*, Fig. S5*B*) and apoptotic cells were not increased in *Lgr5*$^{CreERT2/+}$*;Arid1a*$^{f/f}$ mice (*SI Appendix*, Fig. S5*B*). In addition, immunostaining for GFP showed that Lgr5$^+$ ISCs were comparable between *Lgr5*$^{CreERT2/+}$*-GFP;Arid1a*$^{f/f}$ and control mice at these time points (*SI Appendix*, Fig. S5*B*). These results indicate that *Arid1a* deletion in Lgr5$^+$ ISCs does not perturb homeostasis in the small intestine.

To further confirm the role of Arid1a in Lgr5$^+$ ISCs, we next performed lineage tracing using *Lgr5*$^{CreERT2/+}$*;Rosa26*$^{lacZ/+}$*;Arid1a*$^{f/f}$ mice by crossing *Lgr5*$^{CreERT2/+}$*;Arid1a*$^{f/f}$ mice with *Rosa26*^{lacZ} mice (26). Three days after daily administration of 80 mg/kg tamoxifen for 4 d, lacZ-labeled blue cells appeared as blue stripes from crypts to villi of *Lgr5*$^{CreERT2/+}$*;Rosa26*$^{lacZ/+}$*;Arid1a*$^{f/f}$ mice, that were indistinguishable from control *Lgr5*$^{CreERT2/+}$*; Rosa26*$^{lacZ/+}$*;Arid1*$^{+/+}$ mice (Fig. 3*A*). Three days after the last tamoxifen injection, IHC analysis showed that Arid1a expression was almost lost in the lacZ-labeled blue cells in *Lgr5*$^{CreERT2/+}$*; Rosa26*$^{lacZ/+}$*;Arid1a*$^{f/f}$ mice, confirming the efficient recombination of the floxed *Arid1a*^{flox} allele (Fig. 3*B*); in control *Lgr5*$^{CreERT2/+}$*;Rosa26*$^{lacZ/+}$*;Arid1*$^{+/+}$ mice, lacZ-labeled blue cells represented Arid1a$^+$ expression (Fig. 3*B*). Twenty-one days after the last tamoxifen injection, lacZ-labeled blue cells coinciding with Arid1a expression were observed in control *Lgr5*$^{CreERT2/+}$*; Rosa26*$^{lacZ/+}$*;Arid1*$^{+/+}$ mice, which was similar to the observations on day 3 (Fig. 3 *A* and *B*). Notably, lacZ-labeled blue cells disappeared, and the intestinal epithelial cells including crypts were instead repopulated by lacZ$^-$ Arid1a$^+$ cells in *Lgr5*$^{CreERT2/+}$*; Rosa26*$^{lacZ/+}$*;Arid1a*$^{f/f}$ mice (Fig. 3 *A* and *B*). These results suggest that Arid1a is required for self-renewal and maintenance of ISCs in adult mice.

To further validate these results, we generated *Lgr5-GFP; Villin-Cre;Arid1a*$^{f/f}$ mice, which enabled us to evaluate Lgr5$^+$ ISCs by immunostaining for GFP. Lgr5$^+$ ISCs were observed at the base of crypts in control mice (Fig. 3*C*). In contrast, Lgr5$^+$ ISCs were significantly reduced in the crypts of *Lgr5-GFP;Villin-Cre;Arid1a*$^{f/f}$ mice (Fig. 3 *C* and *D*). In addition, IHC analysis for Musashi-1, a crypt base columnar cell marker, revealed that ISCs were significantly reduced in *Villin-Cre;Arid1a*$^{f/f}$ mice (Fig. 3*E*). This finding was further supported by strikingly decreased expression of ISC markers, including *Lgr5*, *Olfm4*, *Sox9*, *Ascl2*, and *Musashi-1*, in *Villin-Cre;Arid1a*$^{f/f}$ intestines, as determined by q-PCR analysis (Fig. 3*F*). In contrast, q-PCR analysis showed that the expression level of ISC markers, including *Lgr5* and *Ascl2*, was comparable in the large intestine between *Villin-Cre;Arid1a*$^{f/f}$ and *Arid1a*$^{f/f}$ mice (*SI Appendix*, Fig. S1*F*). Taken together, these data indicate that Arid1a is indispensable for the maintenance and self-renewal of Lgr5$^+$ ISCs in the small intestine in mice.

Arid1a Regulates Wnt Signaling Pathway and *Sox9* in the Intestine. To investigate the mechanism underlying the abnormalities, including depletion of Lgr5$^+$ ISCs, shortened villi, and swollen crypts, and increased apoptosis in *Villin-Cre;Arid1a*$^{f/f}$ intestines, we performed genome-wide analysis of gene expression in

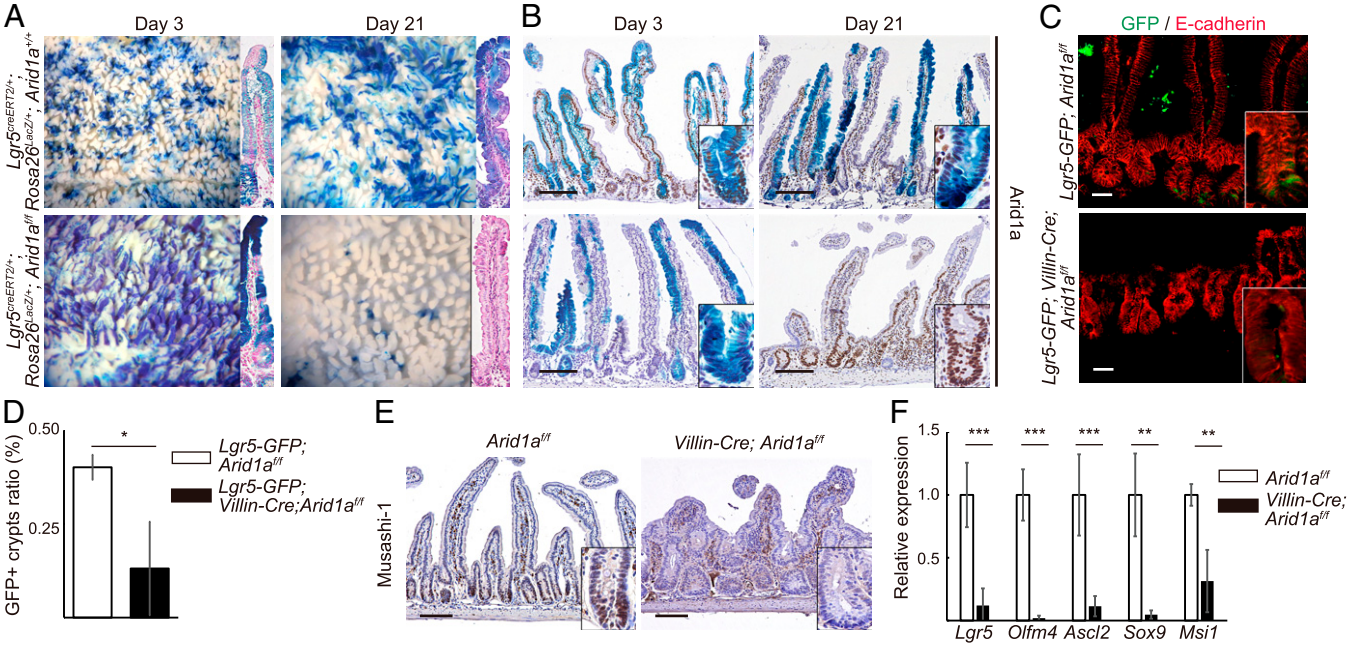

Fig. 3. *Arid1a* deletion leads to loss of ISCs in mice. (*A*) Macroscopic images of staining for LacZ in the small intestine in control (*Upper*) and *Lgr5*$^{CreERT2/+}$*; Rosa*$^{lacZ/+}$*;Arid1a*$^{f/f}$ mice (*Lower*) at 3 and 21 d after the last tamoxifen injection. (*B*) Arid1a and LacZ staining of control (*Upper*) and *Lgr5*$^{CreERT2/+}$*;Rosa*$^{lacZ/+}$*; Arid1a*$^{f/f}$ mice (*Lower*) at 3 and 21 d after the last tamoxifen injection. (*C*) Costaining for GFP/E-cadherin in control (*Upper*) and *Lgr5-GFP;Villin-Cre;Arid1a*$^{f/f}$ mice (*Lower*) at 8 wk of age. (*D*) The percentage of crypts containing at least one GFP$^+$ cell in control and *Lgr5-GFP;Villin-Cre;Arid1a*$^{f/f}$ mice at 8 wk of age (n = 3). (*E*) Musashi-1 staining in the control (*Left*) and *Villin-Cre;Arid1a*$^{f/f}$ mice (*Right*) at 8 wk of age. (*F*) Relative expression levels of ISC markers in control and *Villin-Cre;Arid1a*$^{f/f}$ mice by q-PCR using crypt RNA at 8 wk of age (n = 5). [Scale bars, 50 μm (*C*) and 100 μm (*B* and *E*). The magnification of the right panels of *A* is the same as *B*.] [*Inset* magnification, 2.7× (*B* and *E*) and 1.7× (*C*).] Quantitative data are presented as means ± SD, *P < 0.05, **P < 0.01, ***P < 0.001.

mutant mice. Microarray analysis of mRNA obtained from *Arid1a*$^{f/f}$ and *Villin-Cre;Arid1a*$^{f/f}$ intestines demonstrated that Wnt signaling pathways, including *Wnt3*, *Wnt6*, *Fzd1*, *Fzd2*, *Fzd4*, *Fzd9*, and *Sox9*, which are essential in maintaining intestinal homeostasis (9, 27), were down-regulated in *Arid1a*-deficient intestines relative to *Arid1a*-preserved controls (Fig. 4*A*). As expected, microarray analysis revealed that the expression levels of Paneth cell and ISC markers—including *Mmp7*, *Lyz1*, *Olfm4*, *Ascl2*, *Lgr5*, and *Sox9*—were down-regulated and apoptosis-related genes—including *Hmox1*, *Hif1a*, and *Bcl2*—were up-regulated in *Arid1a*-deficient intestines relative to *Arid1a*-preserved controls (Fig. 4*A*). Furthermore, gene set enrichment analysis (GSEA) on RNA sequence data identified 895 biological processes that were significantly enriched in *Arid1a*-deficient intestines relative to *Arid1a*-preserved controls [false-discovery rate (FDR) set at 0.25]. These processes included a suppressed Wnt signaling pathway and up-regulated apoptosis pathway in *Arid1a*-deficient intestines relative to *Arid1a*-preserved controls (Fig. 4*B*). In addition, q-PCR analysis validated that the expression levels of Wnt target genes—including *Ascl2*, *Sox9*, *Axin2*, *Tcf4*, and *Hes1*—were markedly down-regulated in crypts of *Arid1a*-deficient mice (Figs. 3*F* and 4*C*).

Next, we investigated the expression levels of Wnt agonist and receptor genes that regulate diverse processes of intestinal homeostasis (10–12). Notably, q-PCR analysis revealed that the expression levels of Wnt agonist and receptor genes—including *Wnt3*, *Wnt6*, *Fzd4*, *Fzd5*, *Lrp5*, and *Lrp6*—were also significantly down-regulated in crypts of *Arid1a*-deficient mice (Fig. 4*D*). In addition, the expression level of a Notch ligand, *Dll4*, which is expressed in Paneth cells (14, 28) and is required for intestinal homeostasis (27, 29), was down-regulated in crypts of *Arid1a*-deficient mice (Fig. 4*E*). Various Wnt genes are expressed in diverse cell types of the epithelium and stroma of the murine intestine (15). Recent studies showed that ISCs are supported by Wnts provided from the epithelial or stromal niche cells (16, 30, 31). Interestingly, q-PCR analysis demonstrated that the expression levels of Wnt agonist genes—including *Wnt2b*, *Wnt4*, *Wnt5a*, and *Wnt6*—were strikingly down-regulated in *Arid1a*–deficient intestines (Fig. 4*F*). Consistent with these observations, IHC analysis showed that Sox9 and Hes1 were only faintly expressed in *Villin-Cre;Arid1a*$^{f/f}$ mouse intestines, whereas they were expressed in the crypts of control *Arid1a*$^{f/f}$ mouse intestines (Fig. 4*G* and *SI Appendix*, Fig. S2*C*). These results indicate that the Wnt signaling pathway was strikingly down-regulated in *Arid1a*-deficient intestines.

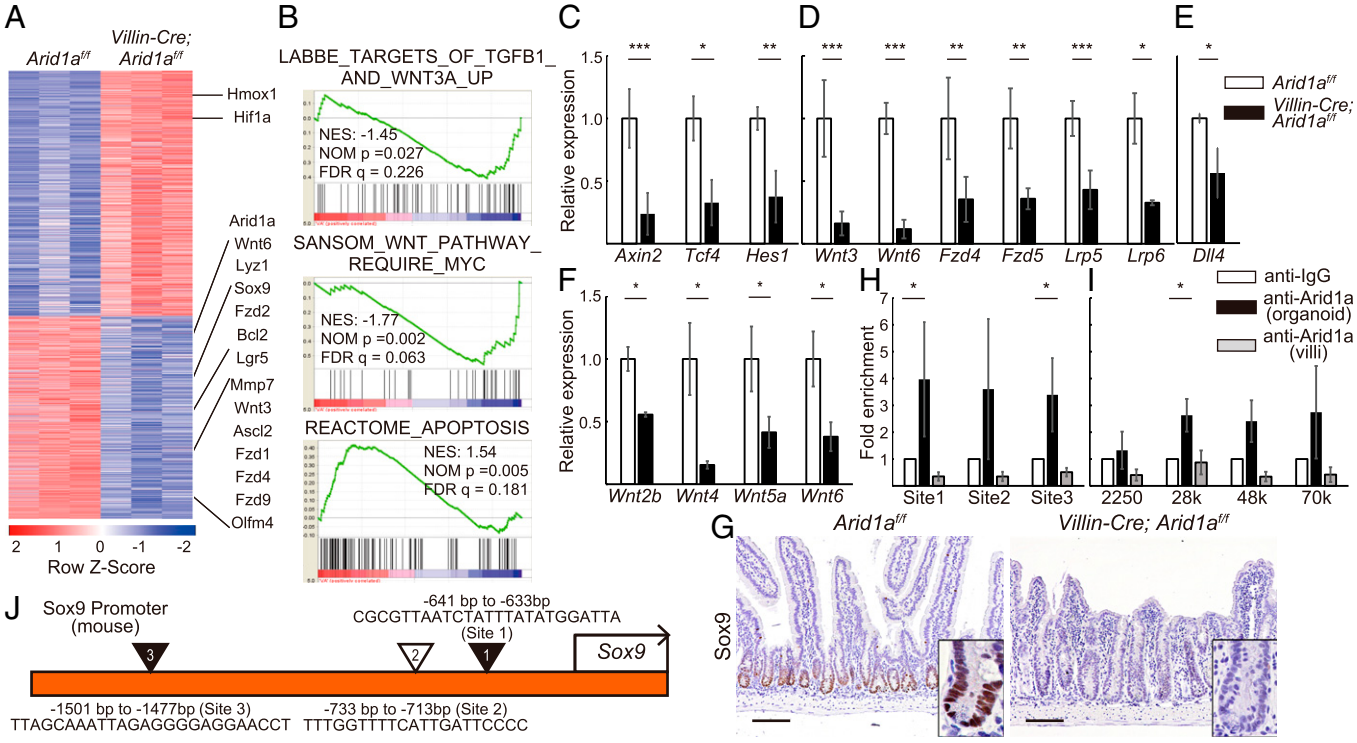

Fig. 4. Intestinal *Arid1a* deletion results in down-regulation of Wnt signaling and Sox9. (*A*) Heatmap of differentially up- and down-regulated genes from RNA-seq using crypt RNA at 8 wk of age ($n = 3$, red is higher, blue is lower expression). (*B*) GSEA shows that Wnt signaling pathway is suppressed and apoptosis pathway is up-regulated in *Villin-Cre;Arid1a*$^{f/f}$ mouse intestines. The LABBE_TARGETS_OF_TGFB1_AND_WNT3A_UP gene set contains up-regulated genes in NMuMG cells (mammary epithelium) after stimulation with both TGFB1 and WNT3A. The SANSOM_WNT_PATHWAY_REQUIRE_MYC gene set contains Wnt target genes up-regulated after Cre-lox knockout of APC in the small intestine that require functional MYC. The REACTOME_APOPTOSIS gene set contains genes involved in apoptosis. Nominal enrichment score (NES), nominal *P* value, and FDR q-value are shown in each GSEA plot. (*C*–*E*) Relative expression levels of Wnt target genes(*C*), Wnt agonist and receptor genes (*D*), and *Dll4* (*E*) in control and *Villin-Cre; Arid1a*$^{f/f}$ mice by q-PCR using crypt RNA at 8 wk of age ($n = 5$). (*F*) Relative expression levels of Wnt agonist genes in control and *Villin-Cre;Arid1a*$^{f/f}$ mice by q-PCR using whole tissue RNA at 8 wk of age ($n = 3$). (*G*) Sox9 staining of *Arid1a*$^{f/f}$ (*Left*) and *Villin-Cre; Arid1a*$^{f/f}$ mice (*Right*) at 8–10 wk of age. (Scale bars, 100 μm.) (*Inset* magnification, 2.7×.) (*H*) Arid1a binding to the *Sox9* promoter regions by ChIP assay using intestinal spheroid cells ($n = 5$) and isolated villous cells ($n = 3$) from wild-type mice at 8 wk of age, respectively. IgG antibody was used as negative control. (*I*) Arid1a binding to the *Sox9* enhancer regions by ChIP assay using intestinal spheroid cells and isolated villous cells from wild-type mice at 8 wk of age ($n = 3$), respectively. IgG antibody was used as a negative control. (*J*) Diagram of the murine *Sox9* promoter sites where Arid1a binds directly (triangles) as investigated by ChIP assay. The black arrow indicates the transcription start site. The black triangles indicate the DNA binding sites (site 1 and site 3) as confirmed by ChIP assay. The white triangle indicates the additional DNA binding site (site 2). Quantitative data are presented as means ± SD, $^*P < 0.05$, $^{**}P < 0.01$, $^{***}P < 0.001$.

Sox9 is required for differentiation of Paneth cells, which provide an epithelial niche for ISCs (14, 19, 20). Given that the expression of *Sox9* mRNA and Sox9 protein was markedly downregulated in crypts of *Arid1a*-deficient mice, we sought to determine whether Arid1a directly binds to the *Sox9* promoter to regulate its expression in the murine intestine. We performed chromatin immunoprecipitation (ChIP) in intestinal spheroid cells that were generated from crypt cells of wild-type mice and discovered that Arid1a binding was enriched at the most proximal and distal site of the Sox9 promoter (denoted sites 1 and 3) (Fig. 4 *H* and *J*). In addition, Arid1a binding tended to be enriched at the second-most proximal site (site 2) and enhancer regions in intestinal spheroid cells, although they did not reach a significant difference (Fig. 4 *H–J*). As negative control, we used IgG antibody, which had minimal binding to chromatin at all of the promoter regions tested. In contrast, we found that Arid1a binding was not enriched at the *Sox9* promoter or enhancer regions in isolated villous cells (Fig. 4 *H* and *I*). Therefore, we concluded that Arid1a binds to the *Sox9* promoter and enhancer regions specifically in the crypt cells in which Sox9 is expressed in the murine intestine.

ChIP-Seq analysis revealed that the top 100 main gene targets for Arid1a in the intestine with minimum *P* values identified by peak calling analysis included many genes that were related to various biological processes or intestinal phenotype (*SI Appendix*, Fig. S6*A*). Furthermore, we also performed Gene Ontology (GO) analysis of all gene targets identified by peak calling analysis. GO analysis implicated that Arid1a directly binds to the regulator genes, which were involved in apoptosis, cell cycle, intestinal epithelial cell differentiation, and the Wnt signaling pathway (*SI Appendix*, Fig. S6*B*). The gene targets for Arid1a in the intestine that regulate the Wnt signaling pathway included *Lrp6*, *Notum*, and *Axin2* (*SI Appendix*, Table S1). In addition, Motif analysis revealed that the top three Arid1a DNA-binding motifs overlap with regulatory motifs recognized by Nr5a2, which regulates differentiation of the pancreas, Foxd3, which is expressed in neural crest precursor cells, and Arid3a, which is a mesenchymal stem cell marker (*SI Appendix*, Fig. S6*C*). This result indicates that Arid1a binds directly to the promoter and enhancer sites of various genes to support their expression. Sequencing coverage histograms showed that coverage that aligned to *Sox9* was similar to coverage that aligned to *Dgkd*. This was one of the Arid1a binding sites, as identified by peak calling analysis with minimum fold-enrichment, although a peak was not identified in the *Sox9* site (*SI Appendix*, Fig. S6*D*).

Taken together, these data indicate that Arid1a regulates the Wnt signaling pathway and Sox9 in the murine intestine, and raise the possibility that the role of *Arid1a* in the maintenance of intestinal homeostasis is mediated by its regulation of the Wnt signaling pathway and Sox9.

Overexpression of *Sox9* Rescues Growth Failure, Disorganized Intestinal Epithelial Architecture, and Increased Apoptosis of Intestinal Cells in *Arid1a*-Deficient Mice. Intestinal deletion of *Sox9* was reported to cause crypt enlargement and decrease of Paneth cells in the intestine (19, 20). Given that these phenotypes observed in intestinal *Sox9*-deleted mice resembled the phenotypes of *Arid1a*-deficient mice, we hypothesized that *Sox9* overexpression could rescue the phenotypes of *Arid1a*-deficient mice. To test this hypothesis, we crossed *SOX9OE* mice (32), in which human *Sox9* is constitutively overexpressed under the control of *Cre* recombinase, with *Villin-Cre;Arid1a*$^{f/f}$ mice to generate *Villin-Cre;Arid1a*$^{f/f}$*;SOX9OE* mice (*SI Appendix*, Fig. S7*A*). The loss of body weight observed in *Villin-Cre;Arid1a*$^{f/f}$ mice was partially rescued in *Villin-Cre;Arid1a*$^{f/f}$*;SOX9OE* mice (Fig. 5*A*), whereas the body weight of *Villin-Cre;Arid1a*$^{f/+}$*; SOX9OE* mice was comparable to that of control *Arid1a*$^{f/f}$ mice (Fig. 5*A*). *Arid1a* was depleted and human *Sox9* was expressed in the intestinal epithelial cells of *Villin-Cre;Arid1a*$^{f/f}$*;SOX9OE* mice, whereas *Arid1a* and human *Sox9* were expressed in the intestinal epithelial cells of *Villin-Cre;Arid1a*$^{f/+}$*;SOX9OE* mice, as confirmed by immunostaining and q-PCR analysis (Fig. 5*B* and *SI Appendix*, Figs. S7 *B–D* and S8*A*). In addition, IHC analysis for GFP confirmed that ectopic Sox9 was entirely expressed in both the villous and crypt epithelial cells in *Villin-Cre;Arid1a*$^{f/f}$*; SOX9OE* and *Villin-Cre;Arid1a*$^{f/+}$*;SOX9OE* mice (Fig. 5*B* and *SI Appendix*, Fig. S8*A*). Notably, histological analysis revealed that the morphological abnormalities, including shortened villi and swollen crypts observed in *Villin-Cre;Arid1a*$^{f/f}$ mouse intestines, were restored in *Villin-Cre;Arid1a*$^{f/f}$*;SOX9OE* intestines (Fig. 5*B*). The length of villi in *Villin-Cre;Arid1a*$^{f/f}$*;SOX9OE* mice was comparable to that of control *Arid1a*$^{f/f}$ mice (Fig. 5*C*). Remarkably, the depth and width of crypts in *Villin-Cre;Arid1a*$^{f/f}$*; SOX9OE* mouse intestines were restored compared with those of *Villin-Cre;Arid1a*$^{f/f}$ mouse intestines (Fig. 5 *D* and *E*), and were comparable to those of control *Arid1a*$^{f/f}$ mouse intestines (Fig. 5 *D* and *E*). We found that the intestinal architecture of *Villin-Cre; Arid1a*$^{f/+}$*;SOX9OE* mice was comparable to that of control *Arid1a*$^{f/f}$ mice (*SI Appendix*, Fig. S8*A*). These results indicate that Sox9 overexpression rescued the growth failure and disorganized architecture of the intestine in *Arid1a*-deficient mice.

We next investigated whether the increased apoptosis was abrogated in *Villin-Cre;Arid1a*$^{f/f}$*;SOX9OE* mouse intestines. Immunostaining and quantitation of cleaved caspase 3 revealed that the number of apoptotic cells in *Villin-Cre;Arid1a*$^{f/f}$*;SOX9OE* mouse intestines was significantly less than that in *Villin-Cre; Arid1a*$^{f/f}$ mouse intestines, and was comparable to that in control *Arid1a*$^{f/f}$ mouse intestines (Fig. 5 *B* and *F*). Furthermore, the apoptotic cells in crypts that were observed in *Villin-Cre;Arid1a*$^{f/f}$ mice were rarely observed in *Villin-Cre;Arid1a*$^{f/f}$*;SOX9OE* mice and were indistinguishable from control *Arid1a*$^{f/f}$ mice (Fig. 5 *B* and *F*), whereas the number of apoptotic cells in *Villin-Cre; Arid1a*$^{f/+}$*;SOX9OE* mice was indistinguishable from that in control *Arid1a*$^{f/f}$ mice (*SI Appendix*, Fig. S8*A*). These data indicate that *Sox9* overexpression offsets increased apoptosis in intestinal *Arid1*a-deficient mice.

***Sox9* Overexpression Reverses Skewed Intestinal Differentiation and Restores Paneth Cells in Intestinal *Arid1a*-Deficient Mice.** We next examined whether the abnormal cellular differentiation observed in *Arid1a*-deficient mice would be reversed in *Villin-Cre;Arid1a*$^{f/f}$*; SOX9OE* mice. Immunostaining and quantification for lysozyme and Mmp7 in *Villin-Cre;Arid1a*$^{f/f}$*;SOX9OE* mice revealed that Paneth cells, which were significantly decreased in *Villin-Cre; Arid1a*$^{f/f}$ mice, were comparable to those in control *Arid1a*$^{f/f}$ mice (Fig. 5 *B* and *G*). The number of goblet cells, one of the secretory cell types, was also restored in *Villin-Cre;Arid1a*$^{f/f}$*; SOX9OE* mice (Fig. 5 *B* and *H*). The numbers of tuft and enteroendocrine cells in *Villin-Cre;Arid1a*$^{f/f}$*;SOX9OE* mice were comparable to those in control *Arid1a*$^{f/f}$ mice, as determined by immunostaining for Dclk1 and chromogranin A, respectively (*SI Appendix*, Fig. S7*E*). We confirmed that cellular differentiation of *Villin-Cre;Arid1a*$^{f/+}$*;SOX9OE* mice was comparable to that of control *Arid1a*$^{f/f}$ mice (*SI Appendix*, Fig. S8*A*). Consistently, q-PCR analysis showed that the expression levels of Paneth cell markers—including *Mmp7*, *Lyz1*, and *Defa6*—were markedly increased in *Villin-Cre;Arid1a*$^{f/f}$*;SOX9OE* mouse intestines compared with *Villin-Cre;Arid1a*$^{f/f}$ mouse intestines, whereas they were dramatically decreased in *Villin-Cre;Arid1a*$^{f/f}$ mouse intestines compared with control *Arid1a*$^{f/f}$ mouse intestines (Fig. 5*I*). Notably, the expression levels of *Wnt3* and *Dll4*, which are produced from Paneth cells and act as essential niche factors in intestinal spheroid cultures (16), were markedly increased in *Villin-Cre;Arid1a*$^{f/f}$*;SOX9OE* mouse intestines compared with *Villin-Cre;Arid1a*$^{f/f}$ mouse intestines (Fig. 5*I*). These results indicate that *Sox9* overexpression reverses skewed intestinal

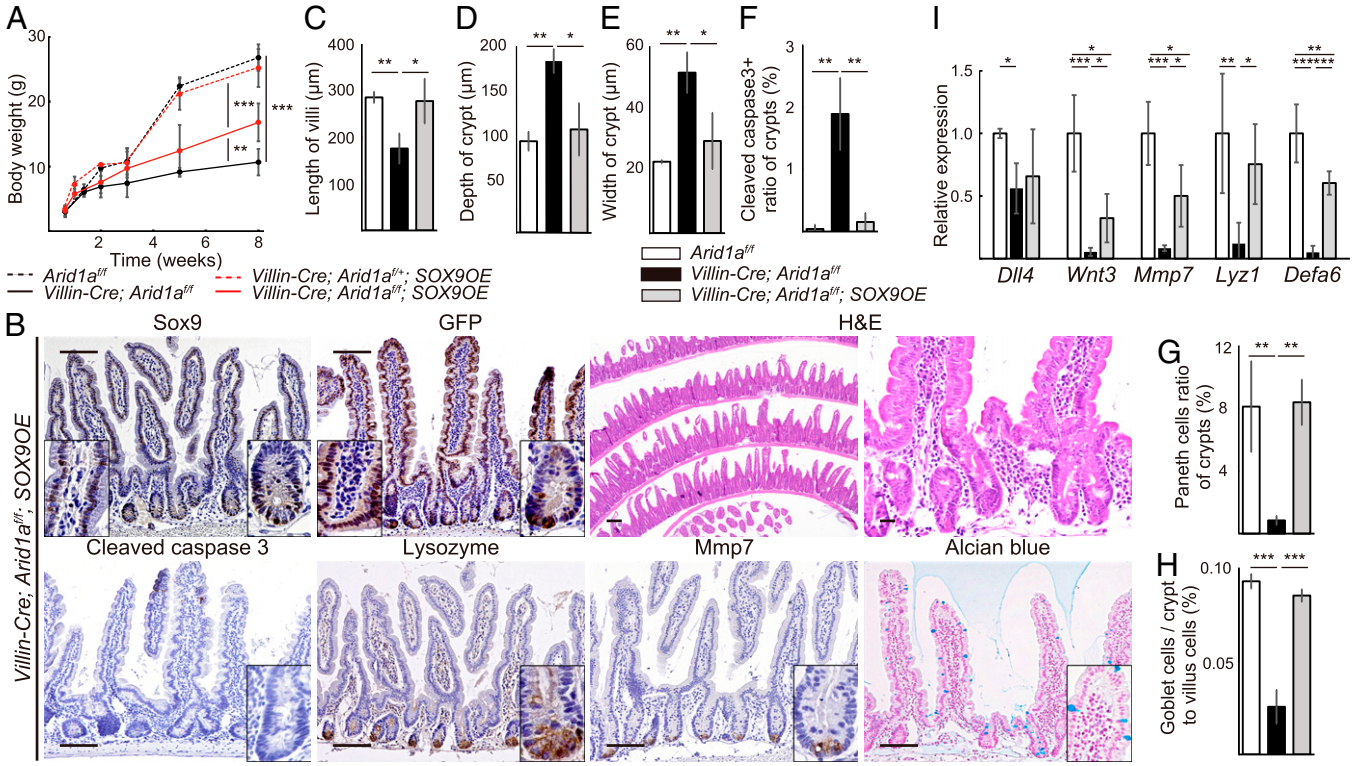

Fig. 5. *Sox9* overexpression rescues growth failure, abnormal intestinal structure, and skewed differentiation in intestinal *Arid1a* mutant mice. (*A*) Body weight at indicated time points for *Arid1a*$^{f/f}$ (black dashed line, $n = 6$), *Villin-Cre;Arid1a*$^{f/+}$*;SOX9OE* (red dashed line $n = 3$), *Villin-Cre;Arid1a*$^{f/f}$ (black line, $n = 6$), and *Villin-Cre;Arid1a*$^{f/f}$*;SOX9OE* mice (red line, $n = 5$). (*B*) IHC analysis for Sox9, GFP, H&E, cleaved caspase 3, lysozyme, Mmp7, and Alcian blue in *Villin-Cre; Arid1a*$^{f/f}$*;SOX9OE* intestines at 8 wk of age. [Scale bars, 50 μm (short) and 100 μm (long).] (*Inset* magnification, 2.7×.) (*C*–*E*) Average length of villi (*C*), depth of crypts (*D*), and width of crypts (*E*) in control, *Villin-Cre;Arid1a*$^{f/f}$ and *Villin-Cre;Arid1a*$^{f/f}$*;SOX9OE* mice at 8–10 wk of age ($n = 3$). (*F*) Ratio of the number of crypts that contained at least one cleaved caspase 3^{+} cell to all crypt numbers in sections from control, *Villin-Cre;Arid1a*$^{f/f}$, and *Villin-Cre;Arid1a*$^{f/f}$*;SOX9OE* mice at 8–10 wk of age ($n = 3$). (*G*) Ratio of the number of Paneth cells to crypt cells in control, *Villin-Cre;Arid1a*$^{f/f}$, and *Villin-Cre;Arid1a*$^{f/f}$*;SOX9OE* mice at 8–10 wk of age ($n = 3$). (*H*) Ratio of the number of Goblet cells to crypt to villus cells in control, *Villin-Cre;Arid1a*$^{f/f}$, and *Villin-Cre;Arid1a*$^{f/f}$*;SOX9OE* mice at 8–10 wk of age ($n = 3$). (*I*) Relative expression levels of Paneth cell markers in control, *Villin-Cre;Arid1a*$^{f/f}$, and *Villin-Cre;Arid1a*$^{f/f}$*;SOX9OE* intestines, as determined by q-PCR using crypt RNA at 8 wk of age ($n = 5$). Quantitative data are presented as means ± SD, $*P < 0.05$, $**P < 0.01$, $***P < 0.001$.

differentiation and restores Paneth cells in *Arid1a*-deficient mouse intestines.

***Sox9* Overexpression Permits Spheroid Development from *Arid1a*-Deficient Intestines.** Given that the development of intestinal spheroids in 3D culture requires ISCs (14, 28), we first tested whether spheroids could be generated from crypts in *Villin-Cre; Arid1a*$^{f/f}$ mice. We tried to isolate intestinal crypts from *Villin-Cre;Arid1a*$^{f/f}$ mice and culture them in vitro; however, spheroids were rarely generated from crypts of *Villin-Cre;Arid1a* mice (Fig. 6 *A* and *B*), further supporting the conclusion that Arid1a is essential for ISCs. To investigate whether the disruption of stem cell maintenance was rescued by *Sox9* overexpression in *Arid1a*-deleted intestines, we tried to generate spheroids from crypts in *Villin-Cre;Arid1a*$^{f/f}$*;SOX9OE* mice. Notably, spheroids were generated from crypts in *Villin-Cre;Arid1a*$^{f/f}$*;SOX9OE* mice, which were comparable to those from crypts in control *Arid1a*$^{f/f}$ mice (Fig. 6*A*). Moreover, the number of spheroids from *Villin-Cre; Arid1a*$^{f/f}$*;SOX9OE* mice was dramatically increased compared with that from *Villin-Cre;Arid1a*$^{f/f}$ mice and was comparable to that from control *Arid1a*$^{f/f}$ mice (Fig. 6*B*), whereas the growth ratio of spheroids from *Villin-Cre;Arid1a*$^{f/f}$*;SOX9OE* mice was still relatively less than that from control *Arid1a*$^{f/f}$ mice (Fig. 6*C*). *Arid1a* deletion and *Sox9* overexpression were confirmed by q-PCR analysis of mRNA derived from spheroids from *Villin-Cre; Arid1a*$^{f/f}$*;SOX9OE* mice compared with those from control *Arid1a*$^{f/f}$ mice (*SI Appendix*, Fig. S7 *F* and *G*). These results suggest that ISCs were restored in *Villin-Cre;Arid1a*$^{f/f}$*;SOX9OE* mice.

***Sox9* Overexpression in Intestinal Epithelial Cells or ISCs Restores Self-Renewal of *Arid1a*-Deficient ISCs.** To further confirm that *Sox9* overexpression restores ISC maintenance in *Arid1a*-deficient ISCs, we performed lineage tracing using *Lgr5*$^{CreERT2/+}$*;Rosa26*$^{lacZ/+}$*; Arid1a*$^{f/f}$*;SOX9OE* mice. Three days after daily administration of 80 mg/kg of tamoxifen for 4 d, lacZ-labeled blue cells appeared as blue stripes from crypts to villi of *Lgr5*$^{CreERT2/+}$*;Rosa26*$^{lacZ/+}$*; Arid1a*$^{f/f}$*;SOX9OE* mice, which were indistinguishable from those in *Lgr5*$^{CreERT2/+}$*;Rosa26*$^{lacZ/+}$*;Arid*$^{+/+}$ and *Lgr5*$^{CreERT2/+}$*; Rosa26*$^{lacZ/+}$*;Arid1a*$^{f/f}$ mice (*SI Appendix*, Fig. S7*H*). Three days after the last tamoxifen injection, IHC analysis revealed loss of Arid1a expression and Sox9 overexpression in the lacZ-labeled blue cells of *Lgr5*$^{CreERT2/+}$*;Rosa26*$^{lacZ/+}$*;Arid1a*$^{f/f}$*; SOX9OE* mice, confirming the efficient recombination of the floxed *Arid1a*^{flox} and *SOX9OE* allele (*SI Appendix*, Fig. S7*H*). Remarkably, 21 d after the last tamoxifen injection, lacZ-labeled blue cells were still observed in *Lgr5*$^{CreERT2/+}$*;Rosa26*$^{lacZ/+}$*;Arid1a*$^{f/f}$*;SOX9OE* mice, which were indistinguishable from *Lgr5*$^{CreERT2/+}$*;Rosa26*$^{lacZ/+}$*; Arid1a*$^{+/+}$ mice (Figs. 3*A* and 7*A*). Again, loss of Arid1a expression was confirmed in almost all lacZ-labeled blue cells in *Lgr5*$^{CreERT2/+}$*; Rosa26*$^{lacZ/+}$*;Arid1a*$^{f/f}$*;SOX9OE* mice (Fig. 7*A*). Quantification revealed that the number of LacZ-labeled crypts was significantly decreased in *Lgr5*$^{CreERT2/+}$*;Rosa*$^{lacZ/+}$*;Arid1a*$^{f/f}$ intestines on day 21 (Fig. 7*B*). Notably, the number of LacZ-labeled crypts in

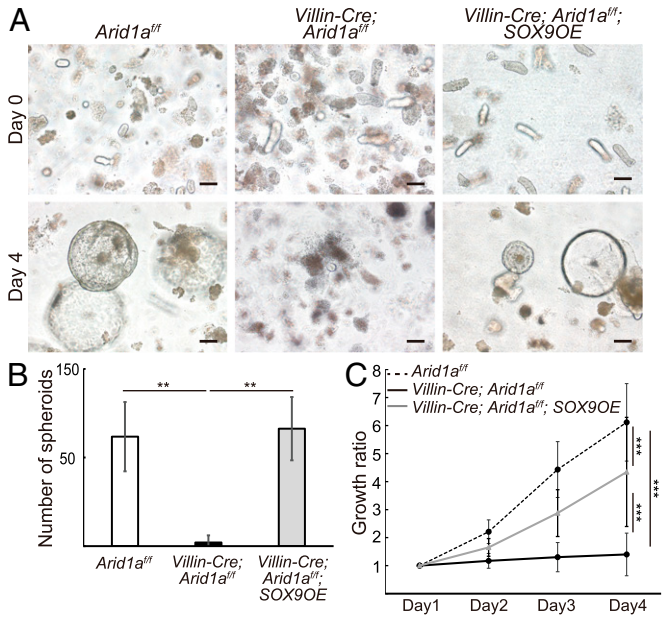

Fig. 6. *Sox9* overexpression permits spheroid development in *Arid1a* mutant mice. (*A*) Time-course images of spheroids generated from crypts in control (*Left*), *Villin-Cre; Arid1a$^{f/f}$* (*Center*), and *Villin-Cre; Arid1a$^{f/f}$; SOX9OE* intestines (*Right*) at 8 wk of age. (Scale bars, 100 μm.) (*B*) The number of spheroids generated from 100 crypts in control (n = 4), *Villin-Cre;Arid1a$^{f/f}$* (n = 30), and *Villin-Cre;Arid1a$^{f/f}$;SOX9OE* intestines (n = 4) at day 4. (*C*) Diameter of spheroids at indicated time points, generated from crypts in control (n = 24), *Villin-Cre;Arid1a$^{f/f}$* (n = 37), and *Villin-Cre;Arid1a$^{f/f}$; SOX9OE* intestines (n = 38). Quantitative data are presented as means ± SD, $^{**}P < 0.01$, $^{***}P < 0.001$.

Lgr5$^{CreERT2/+}$;Rosa$^{lacZ/+}$;Arid1a$^{f/f}$;SOX9OE was comparable to that of control *Lgr5$^{CreERT2/+}$;Rosa$^{lacZ/+}$;Arid1a$^{+/+}$* intestines on day 21 (Fig. 7*B*). These results indicate that *Sox9* overexpression in Lgr5^{+} ISCs restored the self-renewal of *Arid1a*-deficient Lgr5^{+} ISCs. We next performed IHC and q-PCR analysis of ISC markers in crypts of *Villin-Cre;Arid1a$^{f/f}$;SOX9OE* mice. Because GFP represented expression of ectopic Sox9 in *Villin-Cre;Arid1a$^{f/f}$;SOX9OE* mice, we performed IHC analysis for Musashi-1 and Hes1, which are complete blood count cell markers. Immunostaining for Musashi-1 and Hes1 revealed that the position and number of ISCs were comparable between *Villin-Cre;Arid1a$^{f/f}$;SOX9OE* and control *Arid1a$^{f/f}$* mice (Fig. 7*C* and *SI Appendix*, Fig. S7*E*). In addition, the expression levels of ISC markers—including *Lgr5*, *Olfm4*, *Ascl2*, and *Musashi-1*—were partially restored in the crypts of *Villin-Cre;Arid1a$^{f/f}$;SOX9OE* mice compared with control *Arid1a$^{f/f}$* mice (Fig. 7*D*). These results indicate that overexpression of *Sox9* rescues ISC maintenance in intestinal *Arid1a*-deficient mice.

Interestingly, although *Sox9* is a Wnt/Tcf4 target gene, q-PCR analysis demonstrated that the expression levels of other Wnt target genes, including *Tcf4* and *Hes1*, were also up-regulated in *Villin-Cre;Arid1a$^{f/f}$;SOX9OE* mouse intestinal crypts compared with those in *Villin-Cre;Arid1a$^{f/f}$* mice (Fig. 7*E*). In contrast, the expression levels of Wnt agonist and receptor genes—including *Wnt6*, *Fzd4*, *Fzd5*, *Lrp5*, and *Lrp6* except for *Wnt3*—were not restored in crypts of *Villin-Cre;Arid1a$^{f/f}$;SOX9OE* mice compared with those in *Villin-Cre;Arid1a$^{f/f}$* mice (Fig. 7*F*). Furthermore, the expression levels of Wnt agonist genes—including *Wnt2b*, *Wnt4*, *Wnt5a*, and *Wnt6*—were also not restored in *Villin-Cre;Arid1a$^{f/f}$;SOX9OE* intestines compared with those in *Villin-Cre;Arid1a$^{f/f}$* intestines (Fig. 7*G*). We confirmed that the expression levels of stem cell markers, Paneth cell markers, and Wnt receptor genes in *Villin-Cre;Arid1a$^{f/+}$;SOX9OE* mouse intestines were comparable to those in control *Arid1a$^{f/f}$* mouse intestines (*SI Appendix*, Fig. S8 *B–D*). These results suggest that Arid1a regulates the expression of Wnt agonist and receptor genes independently of Sox9.

Discussion

Intestinal deletion of *Arid1a* has been recently reported to spontaneously induce colorectal cancer in mice (8); however, its functional role in intestinal homeostasis remains unclear. In this study, we focused on the specific role of Arid1a in the maintenance of ISCs and intestinal homeostasis in mice. We found that intestinal epithelial deletion of *Arid1a* results in loss of ISCs, increased apoptosis, decreased Paneth and goblet cells, and disorganized crypt-villous structures concomitant with down-regulation of Wnt signaling and Sox9. Remarkably, we showed that Arid1a directly binds to the *Sox9* promoter to regulate its expression and that *Sox9* overexpression in intestinal epithelial cells abrogated the above phenotypes. Moreover, spheroids did not develop from intestinal epithelial cells deficient in *Arid1a*, whereas spheroids developed from *Arid1a*-deficient intestinal epithelial cells concomitant with *Sox9* overexpression. These results indicate that Arid1a is indispensable for the maintenance of ISCs and intestinal homeostasis in mice, which is mainly mediated by Sox9 (*SI Appendix*, Fig. S9*A*).

It is well established that Wnt signaling plays a crucial role in controlling intestinal development and homeostasis (9–12). Indeed, mutation of *Tcf4* leads to depletion of intestinal proliferative compartments in fetal mice, resulting in early death within 24 h after birth (33). In addition, Wnt signaling controls the differentiation of secretory cell lineages in the murine intestine, because overexpression of the Wnt pathway inhibitor, Dickkopf1, blocks the differentiation of secretory cell lineages and leads to shortened villi (34, 35). Wnt signaling also plays an essential role in the maintenance of ISCs (36). Furthermore, intestinal deletion of *Sox9* results in depletion of ISCs concomitant with the loss of Paneth cells and crypt enlargement in mice (14, 19, 20). These previous reports are consistent with our finding that intestinal deletion of *Arid1a* results in loss of ISCs, decreased Paneth and goblet cells, and disorganized crypt-villous structures, concomitant with down-regulation of Wnt signaling and Sox9, which were represented by decreased mRNA expression of Wnt agonists, receptors, and target genes. Similarly, a recent study showed that high-mobility groupA1 chromatin remodeling proteins (Hmga1) up-regulate genes encoding both Wnt agonist receptors and *Sox9* to maintain an ISC niche by expanding the Paneth cell compartment (37). Thus, Arid1a joins a list of genes that play crucial roles in the maintenance of ISCs and a niche for ISCs by regulating Wnt signaling and Sox9.

We previously showed that intestinal deletion of *Brg1*, an ATPase subunit of the SWI/SNF complex, leads to depletion of ISCs in association with down-regulation of Wnt signaling in the neonatal small intestine (5). This observation in *Brg1*-deficient mice is consistent with our findings that ISCs were depleted concomitant with down-regulation of Wnt signaling in *Arid1a*-deleted intestines in this study. In the previous study, β-catenin stabilization did not restore the expression of Wnt signal target genes, and thereby did not rescue ISCs in *Brg1*-deleted intestines. This appears reasonable because Brg1 directly regulates *Tcf2* expression (38, 39). In contrast, it should be noted that *Sox9* overexpression in intestinal epithelial cells restores the maintenance of ISCs and intestinal homeostasis in intestinal *Arid1a*-deleted mice in this study. Interestingly, our data show that *Sox9* overexpression in intestinal epithelial cells did not restore the expression levels of Wnt agonist genes—including *Wnt2b*, *Wnt4*, *Wnt5a*, and *Wnt6*—and receptor genes—including *Fzd4*, *Fzd5*, *Lrp5*, and *Lrp6*—in mice. These results suggest that Arid1a regulates the expression of *Sox9* as well as Wnt agonist and

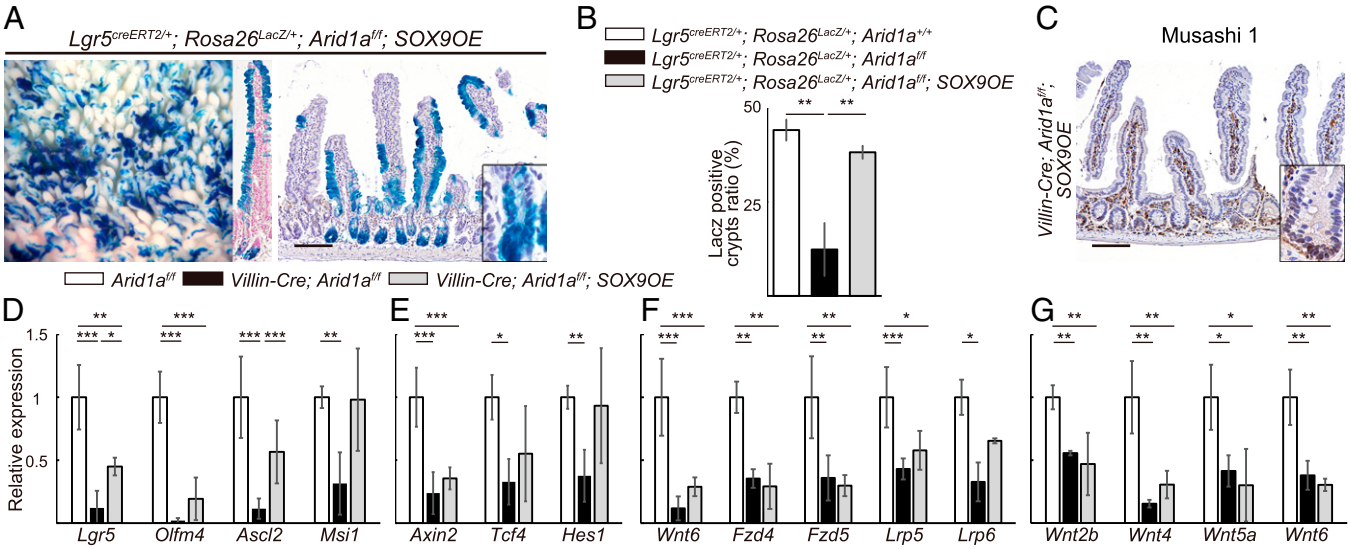

Fig. 7. *Sox9* overexpression restores ISCs in *Arid1a* mutant mice. (*A*) Macroscopic images of staining for LacZ and staining for Arid1a and LacZ in the small intestine in *Lgr5*$^{CreERT2/+}$;*Rosa*$^{lacZ/+}$;*Arid1a*$^{f/f}$;*SOX9OE* mice at 21 d after the last tamoxifen injection. [Scale bar for both panels, 100 μm.] (*Inset* magnification, 2.7×.) (*B*) The percentage of crypts containing at least one LacZ^{+} cell in the control *Lgr5*$^{CreERT2/+}$;*Rosa*$^{lacZ/+}$;*Arid1a*$^{+/+}$, *Lgr5*$^{CreERT2/+}$;*Rosa*$^{lacZ/+}$;*Arid1a*$^{f/f}$, and *Lgr5*$^{CreERT2/+}$;*Rosa*$^{lacZ/+}$;*Arid1a*$^{f/f}$;*SOX9OE* mice at 8 wk of age ($n = 3$). (*C*) Staining for Musashi-1 in *Villin-Cre;Arid1a*$^{f/f}$;*SOX9OE* mice at 8 wk of age. (Scale bar, 100 μm.) (*Inset* magnification, 2.7×.) (*D–F*) Relative expression levels of intestinal stem cell markers (*D*), Wnt target genes (*E*), and Wnt agonist and receptor genes (*F*) in control, *Villin-Cre;Arid1a*$^{f/f}$, and *Villin-Cre;Arid1a*$^{f/f}$;*SOX9OE* intestines by q-PCR using crypt RNA at 8 wk of age ($n = 5$). (*G*) Relative expression levels of Wnt agonist genes in control, *Villin-Cre;Arid1a*$^{f/f}$, and *Villin-Cre;Arid1a*$^{f/f}$;*SOX9OE* intestines by q-PCR using whole tissue RNA at 8 wk of age ($n = 3$). Quantitative data are presented as means ± SD, $*P < 0.05$, $**P < 0.01$, $***P < 0.001$.

receptor genes. It would be interesting to investigate how Arid1a regulates Wnt signaling pathway genes in more detail.

Regarding proliferation, the ratio of the number of K_i67^+ proliferating cells to crypt cells was comparable between *Villin-Cre;Arid1a*$^{f/f}$ and control mice in this study. A previous report showed that the number of proliferating cells in crypts was increased in *Sox9*-deleted intestines, because proliferating cells occupied the entire crypts, including the crypt bottoms where Paneth cells reside in control mice (19). In contrast, overexpression of the Wnt pathway inhibitor, Dickkopf1, results in decreased proliferation (34). Thus, the number of proliferating cells in *Villin-Cre;Arid1a*$^{f/f}$ mice was affected by at least two opposing factors: (*i*) down-regulation of Sox9, which results in increased proliferation, and (*ii*) down-regulation of Wnt agonist and receptors, which results in decreased proliferation.

In this study, we showed that overexpression of *Sox9* in *Arid1a*-deficient mice rescued the phenotype of increased apoptosis, demonstrating that Sox9 mediates apoptosis in *Arid1a*-deficient intestines. Consistently, a previous report showed that intestinal deletion of *Sox9* results in depletion of ISCs (14). Although they did not show whether apoptosis occurs in ISCs of intestinal *Sox9*-deleted mice, it is possible that apoptosis occurs in ISCs, as was observed in intestinal *Arid1a*-deficient mice. Moreover, it was previously reported that *Sox9* knockout results in increased apoptosis in other tissues, including the pancreas and chondrocytes, suggesting an inhibitory role of Sox9 in apoptosis (40, 41). Given that Sox9 regulates apoptosis in villi in *Arid1a*-deficient mice, it is concievable that increased apoptosis due to Sox9 down-regulation contributes to shortened villi in *Arid1a*-deficient mice at least to some extent.

In this study, the expression levels of ISC markers—including *Lgr5*, *Olfm4*, and *Ascl2*—were partially restored in *Villin-Cre;Arid1a*$^{f/f}$;*SOX9OE* intestines, but the restoration was not complete. This result suggests that *Arid1a* deletion has a Sox9-independent effect on intestinal stem cells, which is most likely due to down-regulation of Wnt agonist and receptors in *Arid1a*-deficient intestines. Moreover, the expression levels of Wnt target genes, including *Axin2*, *Tcf4*, and *Hes1* were not completely restored in *Villin-Cre;Arid1a*$^{f/f}$;*SOX9OE* intestines, which is also likely due to the same reason. Furthermore, considering that overexpression of *Sox9* in colon carcinoma cell lines results in down-regulation of Wnt target genes in vitro through a negative feedback (20), it is possible that overexpression of *Sox9* results in down-regulation of Wnt target genes by negative feedback in *Villin-Cre;Arid1a*$^{f/f}$;*SOX9OE* mice. In addition, ChIP-Seq results indicate that Arid1a directly binds to *Lrp6*, *Notum*, and *Axin2* that regulate Wnt signaling pathway. Notum deacylates Wnt proteins and regulates Wnt signaling pathway (42). These data were consistent with our results that some of the Wnt targets (i.e., *Axin2*, and the Wnt ligands/receptors) were not restored in *Villin-Cre;Arid1a*$^{f/f}$;*SOX9OE* intestines.

In this study of lineage-tracing experiments using *Lgr5*$^{CreERT2/+}$ mice, we found that *Arid1a*-deletion in Lgr5^{+} ISCs leads to impaired self-renewal of Lgr5^{+} ISCs, but does not perturb intestinal homeostasis (*SI Appendix*, Fig. S9*B*). It is possible that adjacent transit-amplifying cells or reserve stem cells compensate for the loss of Lgr5^{+} ISCs (43, 44), although further studies are required to corroborate this speculation. It also remains to be clarified whether Arid1a is required for this compensation by neighboring cells.

Interestingly, we showed that deletion of *Arid1a* concomitant with *Sox9* overexpression in Lgr5^{+} ISCs restores self-renewal in *Arid1a*-deleted Lgr5^{+} ISCs (*SI Appendix*, Fig. S9*B*). These results suggest that Arid1a is indispensable for self-renewal of Lgr5^{+} ISCs, which is mediated by its regulation of Sox9. However, it still remains unclear whether Sox9 overexpression in ISCs and Paneth cells precisely restores self-renewal of *Arid1a*-deficient Lgr5^{+} ISCs. We speculate that Arid1a and Sox9 expression in both ISCs and Paneth cells is critical for ISC maintenance. It would be interesting, as a future study, to test this hypothesis using a new transgenic mouse in which CreERT expresses exclusively in Paneth cells.

A previous study showed that intestinal deletion of *Arid1a* leads to spontaneous colorectal cancer development in mice (8).

However, in that previous report, *Villin-CreER^{T2};Arid1a$^{f/f}$;Apc^{Min}* mice had significantly fewer intestinal tumors compared with *Apc^{Min}* mice, and Arid1a expression was retained in the few tumors that did arise in *Villin-CreER^{T2};Arid1a$^{f/f}$;Apc^{Min}* mice (8). These data suggest that *Arid1a* loss drives colon cancer via a mechanism independent of Wnt signaling and that Arid1a is required for Wnt-driven intestinal tumourigenesis (8). This is consistent with our finding that Arid1a is required for activation of Wnt signaling pathway in murine intestines to maintain ISCs and intestinal homeostasis. Given that Brg1 has been shown to have stage- and context-dependent functions in pancreatic tumorigenesis (45), it is reasonable that Arid1a also has context-dependent roles in intestinal tumorigenesis. It would be interesting to investigate how Arid1a plays context-dependent roles in intestinal tumorigenesis in more detail as a future study.

In conclusion, we demonstrated that Arid1a, a component of the SWI/SNF chromatin remodeling complex, is indispensable for the maintenance of ISCs and intestinal homeostasis in mice. These essential roles of Arid1a are mainly mediated by its regulation of *Sox9*. These findings enhance our understanding of intestinal stem cell biology and provide insights into the molecular mechanisms underlying intestinal homeostasis maintenance.

Materials and Methods

Experimental animals were generated by crossing *Villin-Cre* mice (JAX Laboratory #004586), *Lgr5-EGFP-IRES-CreERT2* mice (JAX Laboratory #008875), *Rosa26-lacZ* mice (JAX Laboratory #003309), *Arid1a^{flox}* mice (46), and *SOX9OE* mice (32). Mice were crossed in a mixed background. For induction of Cre-mediated recombination, 80 mg/kg of 20 mg/mL tamoxifen (Sigma-Aldrich) in corn oil, once a day over 4 consecutive days, was injected intraperitoneally. For experiments using normal intestinal tissue, 8- to 10-wk-old mice were used. All experiments were approved by the animal research committee of Kyoto University and performed in accordance with Japanese government regulations. The complete DNA microarray data were deposited in the Gene Expression Omnibus (GEO) at NCBI (www.ncbi.nlm.nih.gov/geo/) with series accession no. GSE110181 (47). The complete ChIP-Seq data were deposited in the Gene Expression Omnibus (GEO) at NCBI (www.ncbi.nlm.nih.gov/geo/) with series accession no. GSE121658 (48).

More detailed descriptions of the methods are available in the *SI Appendix, Materials and Methods*.

ACKNOWLEDGMENTS. We thank Hideyuki Okano for kindly providing the Musashi-1 antibody, Tetsuo Sudo for kindly providing the Hes1 antibody, Yusuke Morita for technical advice for the chromatin immunoprecipitation experiments, Shoko Yokoyama for technical support, and all members of the A.F.–H.S. laboratory for technical assistance and helpful discussions.

1. Workman JL, Kingston RE (1998) Alteration of nucleosome structure as a mechanism of transcriptional regulation. *Annu Rev Biochem* 67:545–579.
2. Hansen JC (2002) Conformational dynamics of the chromatin fiber in solution: Determinants, mechanisms, and functions. *Annu Rev Biophys Biomol Struct* 31:361–392.
3. Chen J, Kinyamu HK, Archer TK (2006) Changes in attitude, changes in latitude: Nuclear receptors remodeling chromatin to regulate transcription. *Mol Endocrinol* 20:1–13.
4. Wilson BG, Roberts CW (2011) SWI/SNF nucleosome remodellers and cancer. *Nat Rev Cancer* 11:481–492.
5. Takada Y, Fukuda A, Chiba T, Seno H (2016) Brg1 plays an essential role in development and homeostasis of the duodenum through regulation of notch signaling. *Development* 143:3532–3539.
6. Dykhuizen EC, et al. (2013) BAF complexes facilitate decatenation of DNA by topoisomerase IIα. *Nature* 497:624–627.
7. Kadoch C, et al. (2013) Proteomic and bioinformatic analysis of mammalian SWI/SNF complexes identifies extensive roles in human malignancy. *Nat Genet* 45:592–601.
8. Mathur R, et al. (2017) ARID1A loss impairs enhancer-mediated gene regulation and drives colon cancer in mice. *Nat Genet* 49:296–302.
9. Scoville DH, Sato T, He XC, Li L (2008) Current view: Intestinal stem cells and signaling. *Gastroenterology* 134:849–864.
10. Clevers H, Nusse R (2012) Wnt/β-catenin signaling and disease. *Cell* 149:1192–1205.
11. Cervantes S, Yamaguchi TP, Hebrok M (2009) Wnt5a is essential for intestinal elongation in mice. *Dev Biol* 326:285–294.
12. Davies PS, Dismuke AD, Powell AE, Carroll KH, Wong MH (2008) Wnt-reporter expression pattern in the mouse intestine during homeostasis. *BMC Gastroenterol* 8:57.
13. Zeve D, et al. (2012) Wnt signaling activation in adipose progenitors promotes insulin-independent muscle glucose uptake. *Cell Metab* 15:492–504.
14. Sato T, et al. (2011) Paneth cells constitute the niche for Lgr5 stem cells in intestinal crypts. *Nature* 469:415–418.
15. Gregorieff A, et al. (2005) Expression pattern of Wnt signaling components in the adult intestine. *Gastroenterology* 129:626–638.
16. Farin HF, Van Es JH, Clevers H (2012) Redundant sources of Wnt regulate intestinal stem cells and promote formation of paneth cells. *Gastroenterology* 143:1518–1529.e7.
17. Blache P, et al. (2004) SOX9 is an intestine crypt transcription factor, is regulated by the Wnt pathway, and represses the CDX2 and MUC2 genes. *J Cell Biol* 166:37–47.
18. Jay P, Berta P, Blache P (2005) Expression of the carcinoembryonic antigen gene is inhibited by SOX9 in human colon carcinoma cells. *Cancer Res* 65:2193–2198.
19. Mori-Akiyama Y, et al. (2007) SOX9 is required for the differentiation of paneth cells in the intestinal epithelium. *Gastroenterology* 133:539–546.
20. Bastide P, et al. (2007) Sox9 regulates cell proliferation and is required for paneth cell differentiation in the intestinal epithelium. *J Cell Biol* 178:635–648.
21. Madison BB, et al. (2002) *Cis* elements of the villin gene control expression in restricted domains of the vertical (crypt) and horizontal (duodenum, cecum) axes of the intestine. *J Biol Chem* 277:33275–33283.
22. Helming KC, et al. (2014) ARID1B is a specific vulnerability in ARID1A-mutant cancers. *Nat Med* 20:251–254.
23. Wilson CL, et al. (1999) Regulation of intestinal alpha-defensin activation by the metalloproteinase matrilysin in innate host defense. *Science* 286:113–117.
24. Gerbe F, et al. (2011) Distinct ATOH1 and Neurog3 requirements define tuft cells as a new secretory cell type in the intestinal epithelium. *J Cell Biol* 192:767–780.
25. Barker N, et al. (2007) Identification of stem cells in small intestine and colon by marker gene Lgr5. *Nature* 449:1003–1007.
26. Soriano P (1999) Generalized lacZ expression with the ROSA26 Cre reporter strain. *Nat Genet* 21:70–71.
27. Pellegrinet L, et al. (2011) Dll1- and dll4-mediated notch signaling are required for homeostasis of intestinal stem cells. *Gastroenterology* 140:1230–1240.e1-7.
28. Sato T, et al. (2009) Single Lgr5 stem cells build crypt-villus structures in vitro without a mesenchymal niche. *Nature* 459:262–265.
29. van Es JH, et al. (2012) Dll1+ secretory progenitor cells revert to stem cells upon crypt damage. *Nat Cell Biol* 14:1099–1104.
30. Kabiri Z, et al. (2014) Stroma provides an intestinal stem cell niche in the absence of epithelial Wnts. *Development* 141:2206–2215.
31. Durand A, et al. (2012) Functional intestinal stem cells after paneth cell ablation induced by the loss of transcription factor Math1 (Atoh1). *Proc Natl Acad Sci USA* 109:8965–8970.
32. Kim Y, et al. (2011) Generation of transgenic mice for conditional overexpression of Sox9. *J Bone Miner Metab* 29:123–129.
33. Korinek V, et al. (1998) Depletion of epithelial stem-cell compartments in the small intestine of mice lacking Tcf-4. *Nat Genet* 19:379–383.
34. Pinto D, Gregorieff A, Begthel H, Clevers H (2003) Canonical Wnt signals are essential for homeostasis of the intestinal epithelium. *Genes Dev* 17:1709–1713.
35. Kuhnert F, et al. (2004) Essential requirement for Wnt signaling in proliferation of adult small intestine and colon revealed by adenoviral expression of Dickkopf-1. *Proc Natl Acad Sci USA* 101:266–271.
36. Sato T, Clevers H (2013) Growing self-organizing mini-guts from a single intestinal stem cell: Mechanism and applications. *Science* 340:1190–1194.
37. Xian L, et al. (2017) HMGA1 amplifies Wnt signalling and expands the intestinal stem cell compartment and paneth cell niche. *Nat Commun* 8:15008.
38. Park JI, et al. (2009) Telomerase modulates Wnt signalling by association with target gene chromatin. *Nature* 460:66–72.
39. Barker N, et al. (2001) The chromatin remodelling factor Brg-1 interacts with beta-catenin to promote target gene activation. *EMBO J* 20:4935–4943.
40. Seymour PA, et al. (2007) SOX9 is required for maintenance of the pancreatic progenitor cell pool. *Proc Natl Acad Sci USA* 104:1865–1870.
41. Akiyama H, Chaboissier MC, Martin JF, Schedl A, de Crombrugghe B (2002) The transcription factor Sox9 has essential roles in successive steps of the chondrocyte differentiation pathway and is required for expression of Sox5 and Sox6. *Genes Dev* 16:2813–2828.
42. Kakugawa S, et al. (2015) Notum deacylates Wnt proteins to suppress signalling activity. *Nature* 519:187–192.
43. Tian H, et al. (2011) A reserve stem cell population in small intestine renders Lgr5-positive cells dispensable. *Nature* 478:255–259.
44. Tetteh PW, et al. (2016) Replacement of lost Lgr5-positive stem cells through plasticity of their enterocyte-lineage daughters. *Cell Stem Cell* 18:203–213.
45. Roy N, et al. (2015) Brg1 promotes both tumor-suppressive and oncogenic activities at distinct stages of pancreatic cancer formation. *Genes Dev* 29:658–671.
46. Gao X, et al. (2008) ES cell pluripotency and germ-layer formation require the SWI/SNF chromatin remodeling component BAF250a. *Proc Natl Acad Sci USA* 105:6656–6661.
47. Hiramatsu Y, Fukuda A (2018) Essential role of Arid1a in intestinal stem cell maintenance and homeostasis through Sox9 regulation. Gene Expression Omnibus. Available at https://www.ncbi.nlm.nih.gov/geo/query/acc.cgi?acc=GSE110181. Deposited February 6, 2018.
48. Hiramatsu Y, Fukuda A (2018) Essential role of Arid1a in intestinal stem cell maintenance and homeostasis through Sox9 regulation (ChIP-Seq). Gene Expression Omnibus. Available at https://www.ncbi.nlm.nih.gov/geo/query/acc.cgi?acc=GSE121658. Deposited October 24, 2018.